*Journal of Structural Geology*, Vol. 1, No. 3, 1979, pp. 181 to 185.

0191-8141/79/0901-0181 $02.00/0

# The geometrical classification of noncylindrical folds

G. D. WILLIAMS

Department of Geology, University College, P.O. Box 78, Cardiff CF1 1XC, Wales

and

T. J. CHAPMAN*

Department of Geology, University of London, Goldsmiths' College, New Cross, London SE14 6NW, England

(*Received* 8 *May* 1979; *accepted in revised form* 14 *August* 1979)

**Abstract** — The majority of naturally occurring folds are noncylindrical if definitions are strictly applied. A new classification of noncylindrical folds using a triangular plot and based on measurements of interlimb angle and hinge angle is proposed. The end-members of the triangular plot are planes, cylindrical isoclines, and isoclinal domes. An infinite range of cylindrical and noncylindrical plane fold shapes may be represented. Noncylindrical nonplane folds may be represented on the plot using proportional circles to signify the degree of non-planarity. The triangular diagram is used to classify large-scale folds from north Norway and their origin is discussed.

## INTRODUCTION

THE GEOMETRICAL description of folded surfaces by structural geologists relies heavily on the analysis of fold profiles within a plane at 90° to the fold axis. A classification of fold profiles based on interlimb angles was given by Fleuty (1964), and more recently, Hudleston (1973) used fourier techniques to describe fold profile shapes. Whilst such two-dimensional descriptions are necessary, they are inadequate for the description of surfaces folded in a complex manner (see Turner & Weiss 1963, p. 108). Noncylindrical folds are those in which not all folded surfaces contain a line parallel to the hinge (Ramsay 1967, p.348). Noncylindrical folds are usually analysed using profile geometries and hinge line orientations over small segments which approach cylindrical form. It seems that naturally occurring folds are rarely cylindrical if the above definition is strictly applied, and many notable examples of noncylindrical folds have been recorded e.g. (Voll 1960, Ramsay 1962, Rhodes & Gayer 1977, Williams & Spray, in press).

In this paper, a simple classification diagram is devised for the description of cylindrical and noncylindrical plane folds (Turner & Weiss 1963, p.108) where the axial surface is planar. A simple modification of the basic diagram allows the representation of non-plane folds where axial surfaces are non-planar, and are themselves folded into cylindrical folds (Turner & Weiss 1963).

## DESCRIPTIVE GEOMETRY OF NONCYLINDRICAL FOLDS

The proposed classification involves the measurement of interlimb angle (Fleuty 1964) within the profile plane, and the measurement of hinge angle within the hinge line surface (Fig. 1a). The hinge angle is that angle subtended by a curved fold hinge line at the points of inflection (Ramsay 1967, p.347) within the hinge line surface (Fig. 1a). An infinite variety of cylindrical plane and noncylindrical plane folds may be described using the two parameters $\alpha$ and $\beta$.

The measurement of the interlimb angle does present a problem. A true profile plane should always be perpendicular to the hinge at any one point, but this

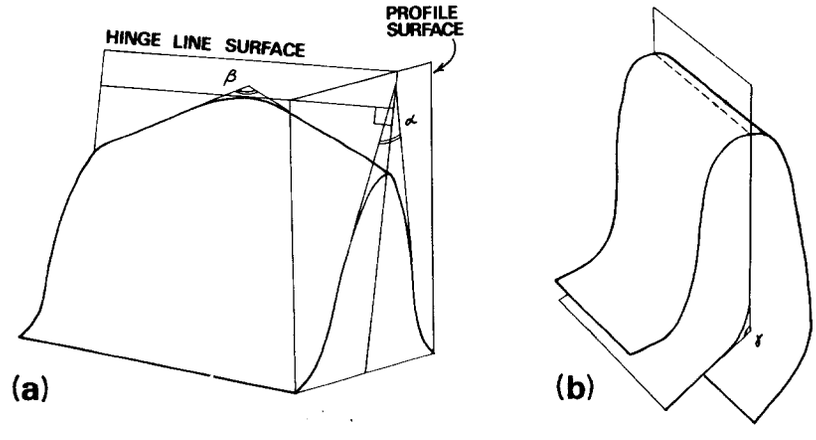


Fig. 1. (a) Geometrical description of a noncylindrical plane fold. $\alpha$ — interlimb angle, $\beta$ — hinge angle. (b) Cylindrical, non-plane fold, $\gamma$– hinge surface angle.

*Present address: Departure of Environmental Sciences, Plymouth Polytechnic, Drake Circus, Plymouth, Devon PL4 8AA.

would involve an infinite number of possible interlimb angles. The present classification does not take this variation into account, but instead a single profile surface is defined as that which is perpendicular to the hinge at the point subtended by the hinge angle β. Although this profile surface may bisect the hinge angle, it does not necessarily do so.

In noncylindrical non-plane folds a third parameter γ is a measurement of the angle subtended by the axial surface at the points of inflection within a plane perpendicular to the axis of curvature of the axial surface (Fig. 1b).

## THE PQR TRIANGULAR DIAGRAM

All noncylindrical plane fold shapes are defined by the two parameters α and β (the interlimb angle and the hinge angle) and the variety of shapes can be represented on a triangular diagram with its apices labelled arbitrarily *P*, *Q* and *R*. A number of conditions must be satisfied before the fold shape can be plotted on the *PQR* diagram; the fold must have a planar hinge line surface and the interlimb angle must be less than, or equal to, the hinge angle. If the hinge angle were less than the interlimb angle it is likely that their roles would have been reversed in the fold description, that is, the hinge angle would be regarded as interlimb angle and vice versa, and thus the condition of $\beta > \alpha$ is satisfied. One further constraint is that no negative values of α and β can be represented; elasticas folds are therefore excluded from the diagram.

In order to plot fold shapes on a triangular diagram, three end members *P*, *Q* and *R* must be calculated and they must show the relationship

$$P + Q + R = 1. \quad (1)$$

One of the conditions for the PQR diagram is that $\beta > \alpha$ and therefore, to provide the shapes illustrated in Fig. 2(a), the values of the end members are:

$$P = \alpha/180, \quad (2)$$

where *P* varies between zero and 1, and represents the degree of planarity of the fold (the reverse of the fold tightness); and

$$R = (180 - \beta)/180, \quad (3)$$

where *R* is the degree of noncylindrism varying between zero for cylindrical folds and 1 for totally noncylindrical folds (isoclinal domes). By rearranging (1) and substituting for P and R:

$$Q = \frac{180 - (\alpha + (180 - \beta))}{180}, \quad (4)$$

where *Q* varies between zero and 1 and represents the degree of domicity. In practice, the relationship expressed in equation 1 means that the position of any fold shape on the *PQR* diagram may be defined by any two of the three parameters. The shapes which can be represented on the *PQR* diagram are shown in Fig. 2 (a), and their descriptive terminology is given in Fig. 2(b). Fold shapes vary infinitely between the three end-members: planes (*P*); cylindrical isoclines (*Q*); and isoclinal domes (*R*). Cylindrical folds with varying degrees of tightness plot along the *PQ* line, the rest of the diagram representing various noncylindrical fold shapes. Isoclinal folds with varying degrees of noncylindrism plot along *QR*, and domes and basins with varying apical angles plot along *PR*.

## REPRESENTATION OF NONPLANE FOLDS ON THE *PQR* DIAGRAM

It is difficult to describe fully the geometrical complexities of noncylindrical nonplane folds as they are surfaces folded about three independent hinges. The angle subtended by the curved axial surface may vary between 180° and 0° for plane folds if the axial surface is folded isoclinally. In this case refolding of the third type described by Ramsay (1967, p.533) would be inferred, each folding episode being analysed separately. The arrangement is included in the present discussion for the sake of completeness.

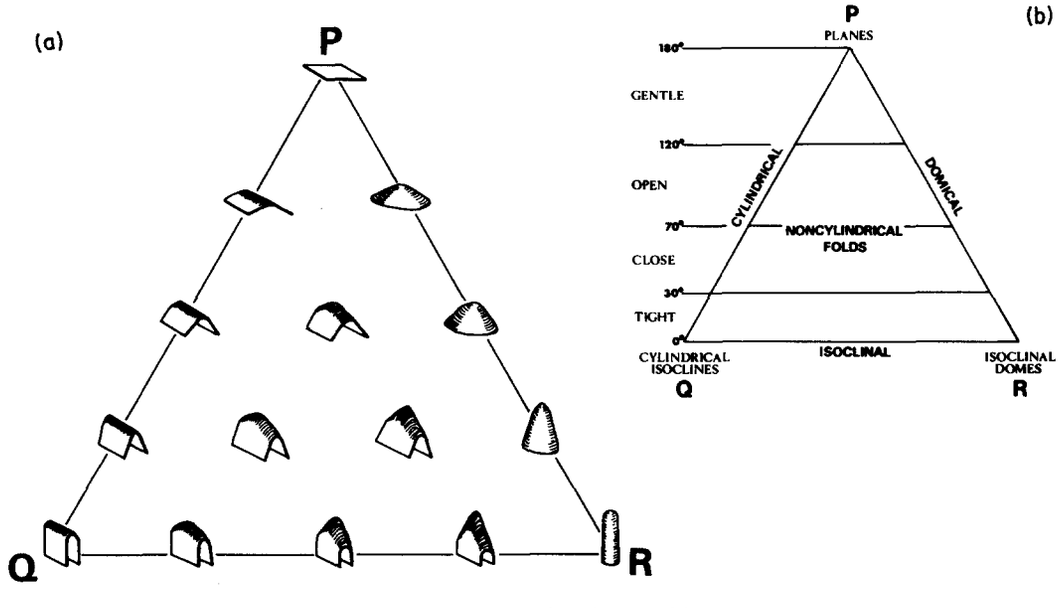


Fig. 2. The variety of fold shapes and their positions on the PQR diagram. (a) Diagramatic representation of fold shapes. (b) Descriptive terminology.

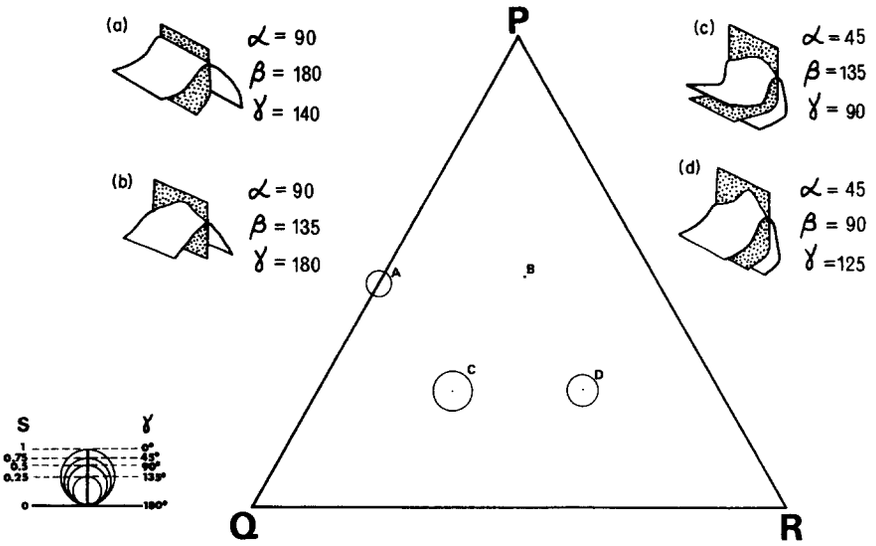


Fig. 3. Modified PQR diagram representing the positions of various non-plane folds. The value of $S$ varies between 0 and 1, and is represented proportionally by the areas of circles, but alternatively can be represented by a proportional bar-scale, or by writing in the angle.

In order to be consistent, the degree of non-planarity of folds should be represented by a parameter which varies between 0 for plane folds and 1 for folds with isoclinally folded axial surfaces. This parameter $S$ is given by

$$S = (180 - \gamma)/180 \quad (5)$$

and it may be portrayed on the basic *PQR* diagram as a circle whose area is proportional to the size of $S$. Alternatively it may be represented by a proportional bar-scale or by writing in the angle $\gamma$. Thus we have a representation of fold shape based on $\alpha$ and $\beta$ values and a visual estimation of the degree of non-planarity (Fig. 3).

## APPLICATIONS OF THE PQR DIAGRAM

The *PQR* diagram may be used to classify individual three-dimensional shapes of cylindrical and noncylindrical folds, and as such, no information is portrayed concerning orientations of structural elements of folds. The recognition and description of noncylindrical folds using eigenvalue methods for the analysis of orientation data has been explained by William & Spray (in press).

Parasitic folds of varying geometry within a single, major fold (e.g. Ramsay & Sturt 1973a,b) could be represented on the *PQR* diagram, and may plot in

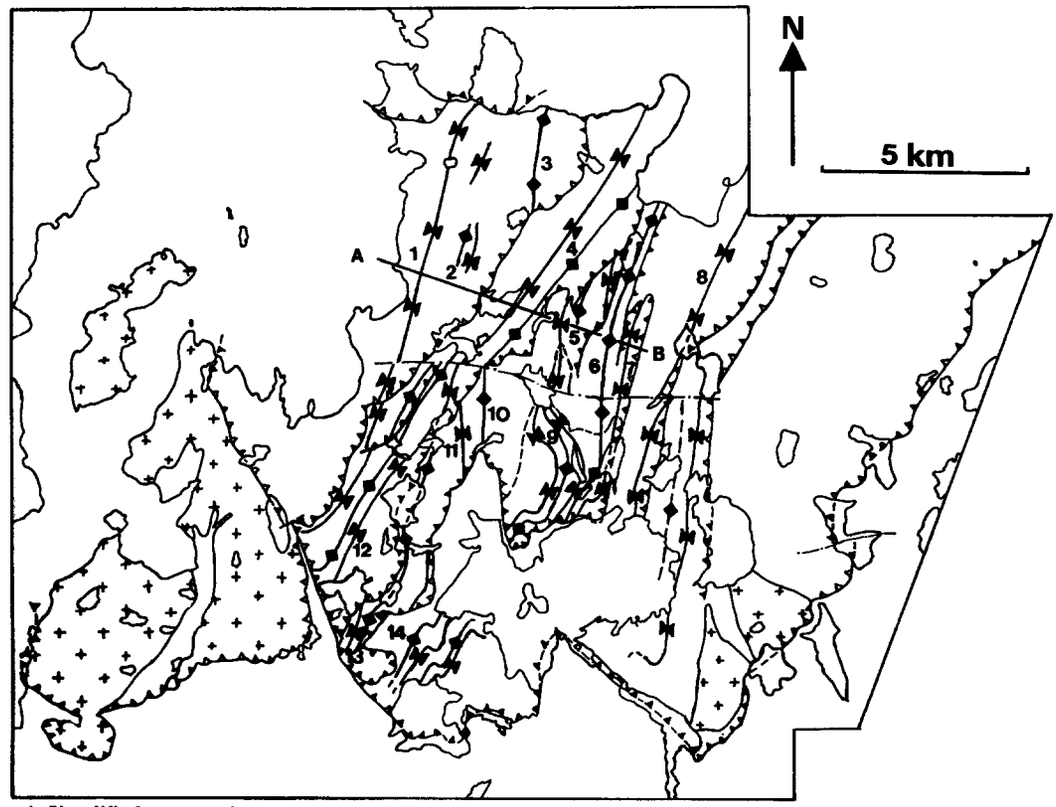


Fig. 4. Simplified structural map of the Laksefjord Nappe complex, showing the major $F_1$ fold axial traces. Large-scale $F_2$ folds which are restricted to the south, refold the $F_1$ folds. These are omitted for clarity. North of line *A–B* folds 1,4,5 and 6 have sub-horizontal plunges, but south of the lines plunge steepens to the south or southwest. Numbers refer to the folds plotted on the PQR diagram (Fig. 6) Crossed ornament-basement within Laksefjord Nappe; teeth—thrusts; pecked-dotted lines—faults.

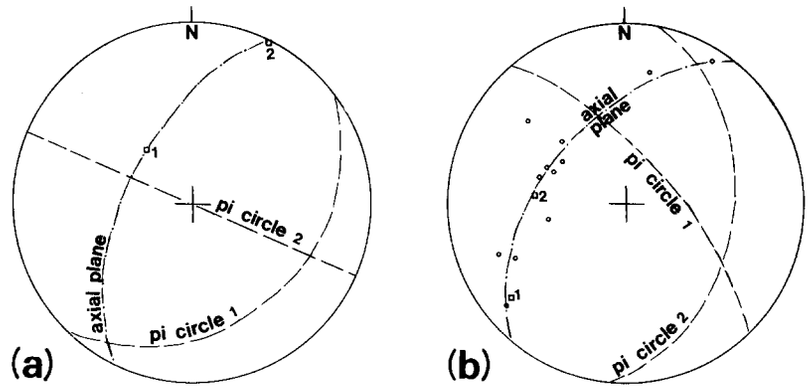


Fig. 5. (a) Simplified structural data for fold 1, pi circle and axis 1 from south of the line *A–B* in Fig. 4, pi circle and axis 2 from north of the line *A–B* in Fig 4. Axial surface and $S_1$ foliation — pecked — dotted line great circle. (b) Simplified structural data for fold 4. pi circle and axis 1 from north of line *A–B* in Fig 4, pi circle and axis 2 from south of line *A–B*. Circles are intersection lineations of bedding on the $S_1$ foliation.

significantly different fields. On a regional scale, inhomogeneous strain could give rise to varying degrees of fold tightness and noncylindrism (see Rhodes & Gayer 1977) which should be discernable using the *PQR* plot. Also, on a large scale, major individual folds, especially domical shapes, could be represented if $\alpha$ and $\beta$ were calculated from maximum hinge plunges and limb dips shown on geological maps.

## NATURAL FOLDS FROM NORWAY AND THEIR REPRESENTATION ON THE PQR DIAGRAM

The Laksefjord Nappe complex (Føyn 1960) forms the middle nappe in the Caledonian overthrust belt of Finnmark. The rocks are lower greenschist facies metasediments and within a large middle thrust unit there are quartzites, pelites and a lower conglomeratic unit. Crystalline basement rocks and carbonates form the lowest thrust sheet of the complex whilst pelites form the upper thrust unit. Five deformational episodes are recognisable.

Within the middle and most extensive thrust unit (itself formed of a number of thrust slices) large-scale $F_1$ folds and post-$F_1$ pre-$F_2$ thrusts are largely responsible for the present structure and distribution of rock types (Fig. 4). Large-scale $F_2$ folds are confined to the southern part of the nappe. The large-scale $F_1$ folds vary from open within the quartzitic units to isoclinal in the phyllites. Wavelengths vary from 0.2 to 2.0 km. A well developed penetrative $S_1$ foliation is axial planar to the folds.

Whilst the $F_1$ folds are reasonably cylindrical with low angle plunges over several kilometres, several show a marked change in axial plunge at certain places, from 0° to over 50°.

Detailed mapping and structural analysis indicate that this variation in axial plunge is an original noncylindrism of the folds. The evidence for this follows. The different axial plunges for one fold are contained within a single axial plane. For example, in fold 1 in the north the plunge is 026/00 whilst in the south it becomes 320/57 (Fig. 5a). This is an angular variation through 78°. Both axes are contained within a single plane, the axial plane, to which in both cases $S_1$ is subparallel. Within the phyllites of folds 4 (two isoclinal folds) a variation through 46° within the axial plane results in the fold axis plunging 230/20 (i.e. to the SW) in the north but at 280/50 (i.e. to the WNW) in the south (Fig. 5b). This means the fold axis actually 'overturns' within the axial plane. The latter is defined by an $S_1$ foliation (commonly parallel to bedding) which remains remarkably constant in orientation throughout the area. A further important feature is that an array of intersection lineations of bedding on $S_1$ surfaces plots on the same great circle (Fig. 5b). Refolding cannot account for these relationships, so the folds must have a primary noncylindrism. Because the axial surfaces are planar throughout, the folds are noncylindrical plane folds (Turner & Weiss 1963). It should be noted that the slight curving towards the east in some of the N–S trending $F_1$ folds at their northern extremities is due to a slight $F_2$ rotation. This has resulted in some axial planes being gently flexed but makes little difference to the primary shape of the $F_1$ folds.

The numbered $F_1$ folds in Fig. 4 have been plotted on a *PQR* diagram (Fig. 6). The most obvious feature is the three separate fields which clearly indicate the control exerted by lithology in fold cores on tightness. The field

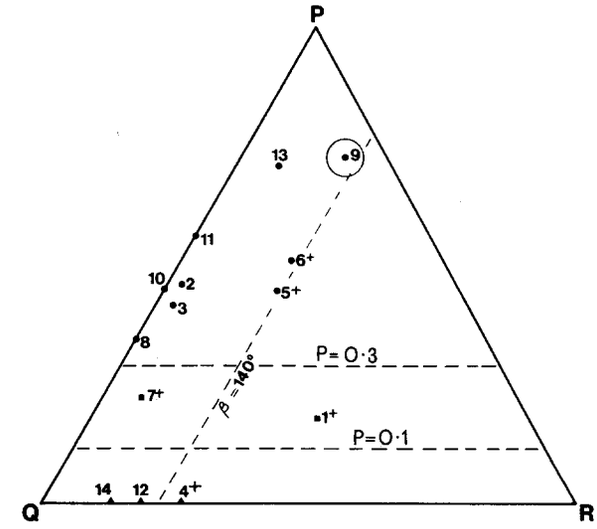


Fig. 6. PQR diagram for the numbered $F_1$ folds in Fig. 4. Circles — folds with quartzites or massive quartz rich metasiltstones in their cores. Squares—folds with interbedded quartzites and pelite in their cores. Triangles—folds within pelites only. Crosses— folds with marked change in plunge along line *A–B* in successive thrust sheets.

for folds with quartzites or massive meta-siltstones in their cores lies between $P$ values of 0.1 and 0.3; that for interbedded lithologies between 0 and 0.1; and that for pelites approaches $P$ values of 0.

There also appears to be, with one exception, a fairly well-defined maximum degree of noncylindrism at $\alpha = 140°$ with an $R$ value of 0.22.

Folds 9 (actually three folds) are apparently the only primary non-plane noncylindrical folds in the region. They have been 'pinched' in tightly around the open core of fold 6, an anticline in thick-bedded quartzites. The axis of curvature of the axial plane is nearly vertical, at about 90° to the fold axis.

## A POSSIBLE ORIGIN FOR THE NONCYLINDRICAL PLANE $F_1$ FOLDS

A clue to their origin may lie in the position of change of the axial plunges of folds 1,4,5 and 6. The folds lie within three successive thrust sheets. Furthermore, their respective positions of change in axial plunge (i.e. the 'hinges' of the hinge angle $\beta$) lie in a straight line trending WNW (line $A$–$B$ in Fig. 4). North of this line the folds have a gentle plunge, whilst south of it they plunge steeply to the south or southwest. The direction of this line is remarkably close to the average extension lineation direction for the first deformation in the middle unit of the nappe complex.

If the $F_1$ folds were initiated before thrusting (the thrusts truncate $F_1$ folds) but during nappe translation they continued to tighten and developed a penetrative foliation, it is possible that the uneven topography over which the nappe was travelling, might be able to transmit its irregularities through to each successive sheet. It is probable that the extension lineation is parallel to the direction of nappe translation and hence as each successive sheet passed over a topographical irregularity the effect of this irregularity may have been transmitted upward through the sheets along lines parallel to the transport direction. The tightening and flattening of the folds and the schistosity development would have to take place whilst or after they had moved over a topographical feature in order to preserve the variation in axial plunge within a planar axial surface. The maximum $R$ value of 0.22 ($\alpha = 140$) may be a reflection of the topographic irregularity of the underlying surface.

*Acknowledgements* — R. A. Gayer kindly read and criticised the manuscript. Fieldwork was carried out under the tenure of a N.E.R.C. studentship.

### REFERENCES

Fleuty, M. J. 1964. The description of folds. *Proc. Geol. Ass.* **75,** 461–492.

Føyn, S. 1960. Tanafjord to Laksefjord. *Guide to Excursion A3, 21st Int. geol. Congr. Copenhagen,* 45–55.

Hudleston, P. J. 1973. Fold morphology and some geometrical implications of theories of fold development. *Tectonophysics* **16,** 1–46.

Ramsay, D. M. & Sturt, B. A. 1973a. An analysis of noncylindrical and incongruous fold pattern from the Eocambrian rocks of Sørøy, Northern Norway. 1. Noncylindrical, incongruous and abberrant folding. *Tectonophysics* **18,** 81-107.

Ramsay, D. M. & Sturt, B.A. 1973b. An analysis of noncylindrical and incongruous fold pattern from the Eocambrian rocks of Sørøy, Northern Norway. 2. The significance of the synfold stretching lineation in the evolution of noncylindrical folds. *Tectonophysics* **18,** 109–121.

Ramsay, J. G. 1962. The geometry and mechanics of formation of similar type folds. *J. Geol.* **70,** 309–327.

Ramsay, J. G. 1967. *Folding and Fracturing of Rocks.* McGraw-Hill, New York.

Rhodes, S. & Gayer, R. A. 1977. Noncylindrical folds, linear structures in the $X$ direction and mylonite developed during translation of the Caledonian Kalak Nappe Complex of Finnmark. *Geol. Mag.* **114,** 329–341.

Turner, F. J. & Weiss, L. E. 1963. *Structural Analysis of Metamorphic Tectonites.* McGraw-Hill, New York.

Voll, G. 1960. New work on petrofabrics. *Lpool Manchr geol. J.* **2,** 503–567.

Williams, G. D. & Spray, J. G. in press. Noncylindrical, flexural-slip folding in the Ardwell Flags – a statistical approach. *Tectonophysics.*